

Finite Element Analysis of Earth Retention System with Prestressed Wales

프리스트레스트 띠장을 적용한 흙막이 시스템의 유한요소해석

Park, Jong-Sik¹

박 종 식

Kim, Sung-Kyu²

김 성 규

Joo, Yong-Sun³

주 용 선

Kim, Nak-Kyung⁴

김 낙 경

요 지

프리스트레스트 띠장을 적용한 새로운 흙막이 시스템에 대한 유한요소 해석이 수행되었다. 본 연구에서는 프리스트레스트 띠장을 적용한 흙막이 시스템의 거동을 규명하기 위하여 3 차원 유한요소 모델이 적용되었다. 새로운 흙막이 시스템에 대한 유한요소 모델링 절차와 방법이 제시되었다. 지반, 벽체, 버팀보 및 프리스트레스트 띠장 시스템을 구성하고 있는 띠장, 받침대, 강선에 대한 모델링과 지반-벽체 그리고 벽체-띠장 간의 접촉면 모델링이 제시되었다. 벽체 횡방향 변위, 버팀보 축력, 프리스트레스트 띠장 시스템 부재인 띠장과 받침대 축력에 대한 유한요소 해석결과가 현장 계측결과와 비교 검증되었다. 검증된 3 차원 유한요소 모델을 이용하여 강선 인장력 변화에 따른 새로운 프리스트레스트 띠장의 휨모멘트와 변형 거동이 규명되었으며 이에 따른 흙막이 벽체 배면에 서의 토압 거동이 규명되었다.

Abstract

A finite element analysis was performed for new earth retention system with prestressed wales. A 3D finite element model was adopted in this study to investigate the behavior of the earth retention system with prestressed wales. A procedure of the 3D finite element modeling of this earth retention system was presented. The procedure included the modeling of soil, wall, strut, and members of prestressed wale system which consists of wale, support leg, and steel wires, and the interface modeling of soil-wall and wall-wale. The numerical predictions of lateral wall deflection, and axial load on the members of prestressed wale systems and struts were evaluated in comparison with the measurements obtained from field instruments. A sensitivity analysis was performed using the proposed 3D finite element model to investigate the behavior of new earth retention system on a wide range of prestress load conditions of steel wires. The lateral deflection of the wall and wale, the bending moment of the wale, and the lateral earth pressure distribution on the wall were computed. Implications of the results from this study were discussed.

Keywords : Earth retention system, Excavation, Finite element analysis, Prestressed wale

1 Member, Senior Researcher, Hanwha Research Institute of Technology

2 Member, Graduate Student, Dept. of Civil, Architect. Envir. System Engrg., Sungkyunkwan Univ.

3 Member, Graduate Student, Dept. of Civil, Architect. Envir. System Engrg., Sungkyunkwan Univ.

4 Member, Assoc. Prof., Dept. of Civil, Architectural and Envir. System Engrg., Sungkyunkwan Univ., nkkim@skku.edu, Corresponding Author

1. Introduction

A new earth retention system with prestressed wales was developed and introduced as an alternative method for conventional temporary earth support systems as braced cuts and anchored walls (Han et al. 2003a; Kim et al. 2004). A new wale system is a wale prestressed by tensioning steel wires. The newly prestressed wale system consists of wales, H-beam support legs, steel wires, and hydraulic jacks, as shown in Fig. 1. The newly prestressed wale system provides a highly flexural resistance against a bending by lateral earth pressures. A new earth retention system with prestressed wales provides the spacing of supports drastically larger than those of conventional temporary support systems. The new earth retention system can reduce the quantity of steel beams than conventional braced cuts. Therefore, large workspace provides construction easiness. The prestressed wale system has a preloading effect on the wall, and the preload restricts the wall deformation due to ground excavation.

The new earth retention system with prestressed wales in excavations for buildings, water lines, bridge piers, subway structures performed successfully. There have been studies on the new earth retention system with prestressed wales by Han et al. (2003b), Kim et al. (2005a), Kim et al. (2004, 2005b,c), Kim et al. (2005d), and Park et al. (2003a,b, 2004). The basic principles and design method of new earth retention system with prestressed wales were investigated by Han et al. (2003b), Kim et al. (2004), and Park et al. (2003a,b). The applicability and safety of the new earth retention system in a variety of field excavations were investigated and discussed by Kim et al. (2004, 2005b,c). The stability of the new prestressed wale system was evaluated by the finite element approach by Kim et al. (2005a). The

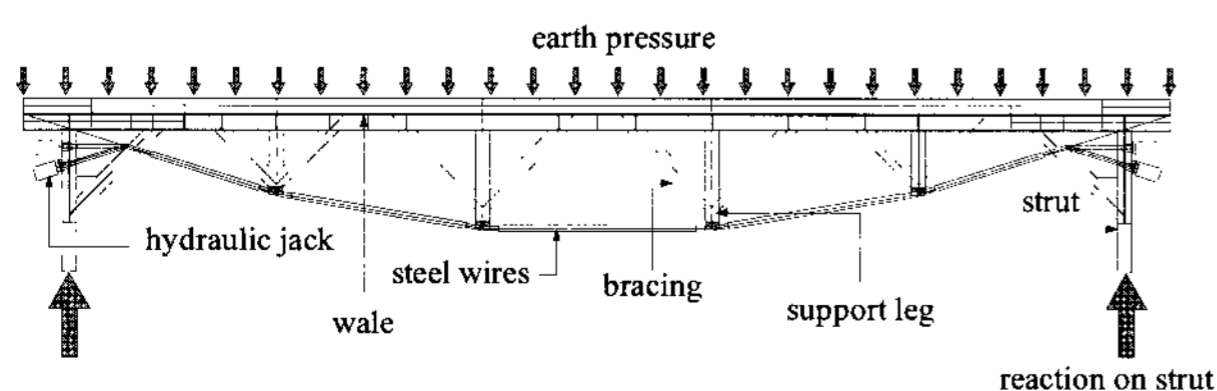


Fig. 1. Components of new prestressed wale system

structural behavior of this prestressed wale system applied in the earth retention system in soft clay was studied by Kim et al. (2005d). A modeling technique for this prestressed wale system was proposed by Kim et al. (2005a).

A numerical analysis of the new earth retention system with prestressed wales was performed using the finite element method. A 3D finite element model was adopted to investigate the behavior of the wall and newly prestressed wales in excavation. The modeling of soil, wall, strut, and prestressed wale system members, and the interface modeling of soil-wall and wall-wale were presented in this paper. The numerical predictions of lateral wall deflection, and axial load on the members of prestressed wale systems and struts were evaluated compared with the measured data from field monitoring. In order to investigate the behavior of the new earth retention system on the effect of prestress load conditions of steel wires, a series of finite element analyses were performed using the proposed 3D finite element model. The lateral deflection of the wall and wale, the bending moment of the wale, and the lateral earth pressure distribution on the wall were computed. The implications of the results were discussed.

2. New Earth Retention System with Prestressed Wales in Urban Excavation

2.1 Site Conditions

The new earth retention system with prestressed wales was selected for temporary earth support in apartment complex building in Anyang area. The excavation was 48 meters wide, 44 meters long, and 11.9 meters deep. The old houses and stores were located in the vicinity of the site. The subsurface soil consists of fill, silty clay with sand, weathered soil, and weathered rock. The construction site map, geologic map, boring locations, subsurface soil distribution, and SPT profiles of the excavation site are reported by Kim et al. (2005b) in detail.

2.2 Excavation Support System

The CIP wall is internally braced with three levels of prestressed wales and preloaded corner struts. LW grouting was used to prevent the inflow of the ground water. Details of the CIP wall, the prestressed wale systems and corner struts used in the excavation and conditions of the prestresses on steel wires of the wale systems and the preloads of corner struts are reported by Kim et al. (2005b). And the construction sequence and field monitoring plan for the new earth retention system with prestressed wales are presented by Kim et al. (2005b). The new earth retention system with prestressed wales in urban excavation performed successfully, as shown in Fig. 2.

3. Three Dimensional Finite Element Analysis of Earth Retention System with Prestressed Wales

A three-dimensional finite element analysis was performed for the new earth retention system with prestressed wales. Details of the finite element modeling of this earth retention system were presented. The numerical predictions of the lateral wall deflection, and axial loads of the wale, support leg, and strut were evaluated and compared with the field measurements.



Fig. 2. New Earth Retention System with Prestressed Wales in Urban Excavation

3.1 Finite Element Model

3.1.1 Mesh Boundary Condition

An idealized 3D mesh, which consists of 88,440 nodes and 71,664 elements, was generated to minimize the effect of mesh size effect on the finite element analysis, as shown in Fig. 3. Based on studies proposed by Briaud and Lim (1999), and Yoo (2001), and on a previous study for boundary effect on this 3D finite element analysis, the mesh boundaries were defined in Fig. 4. The finite element mesh of the wall and prestressed wale systems is shown in Fig. 5. The depth of excavation H was 12.0 m. The distance from the bottom of the excavation to the hard layer D_b was $1.2H$. The 3D mesh extended laterally to a distance of $4.0H$ from the vertical excavation surface.

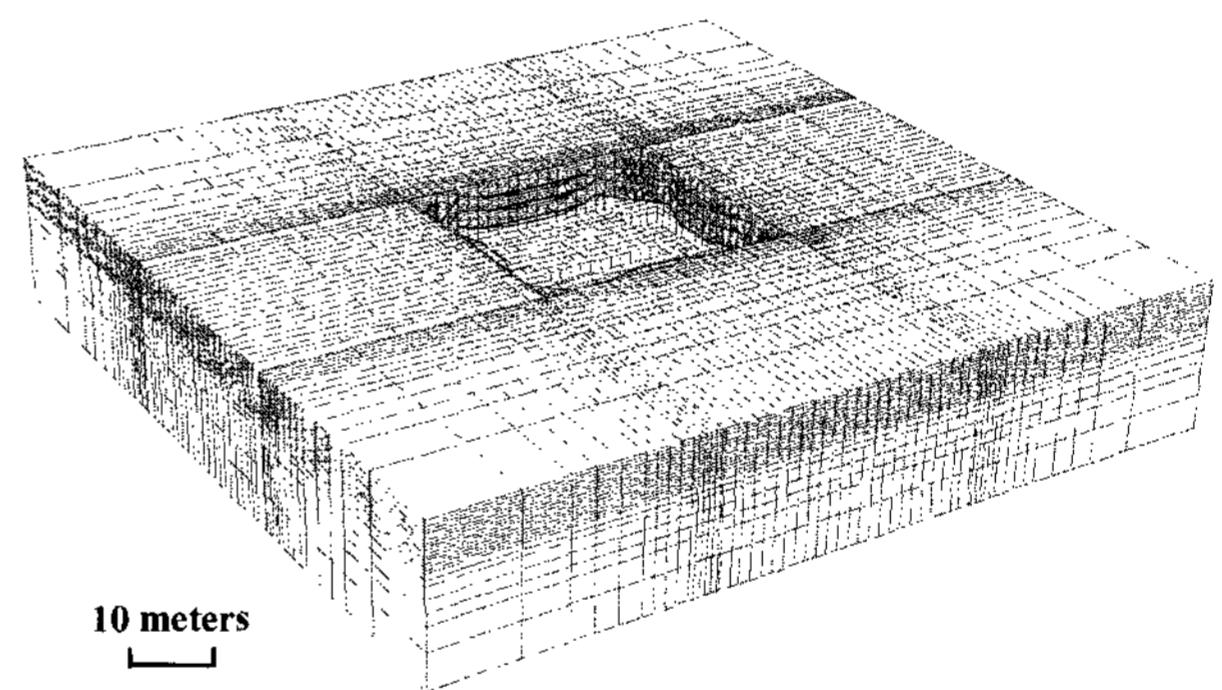


Fig. 3. 3D finite element mesh

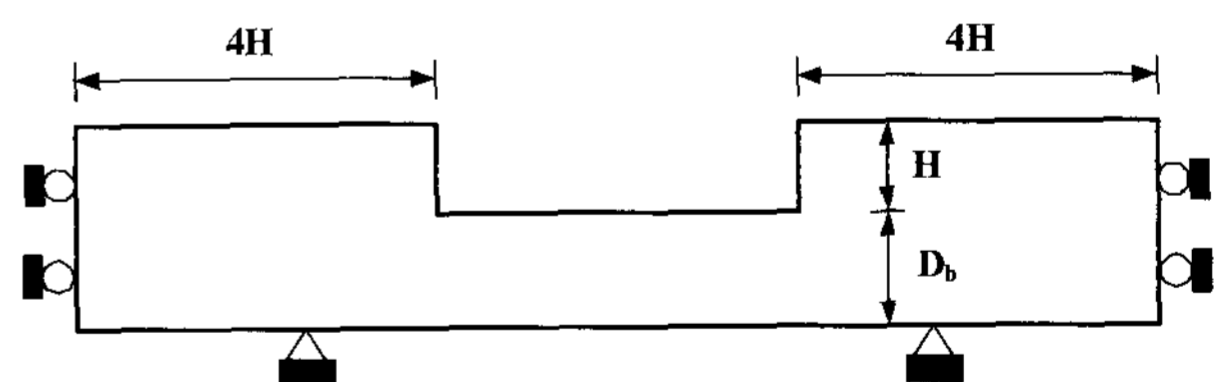


Fig. 4. Definition of mesh boundaries

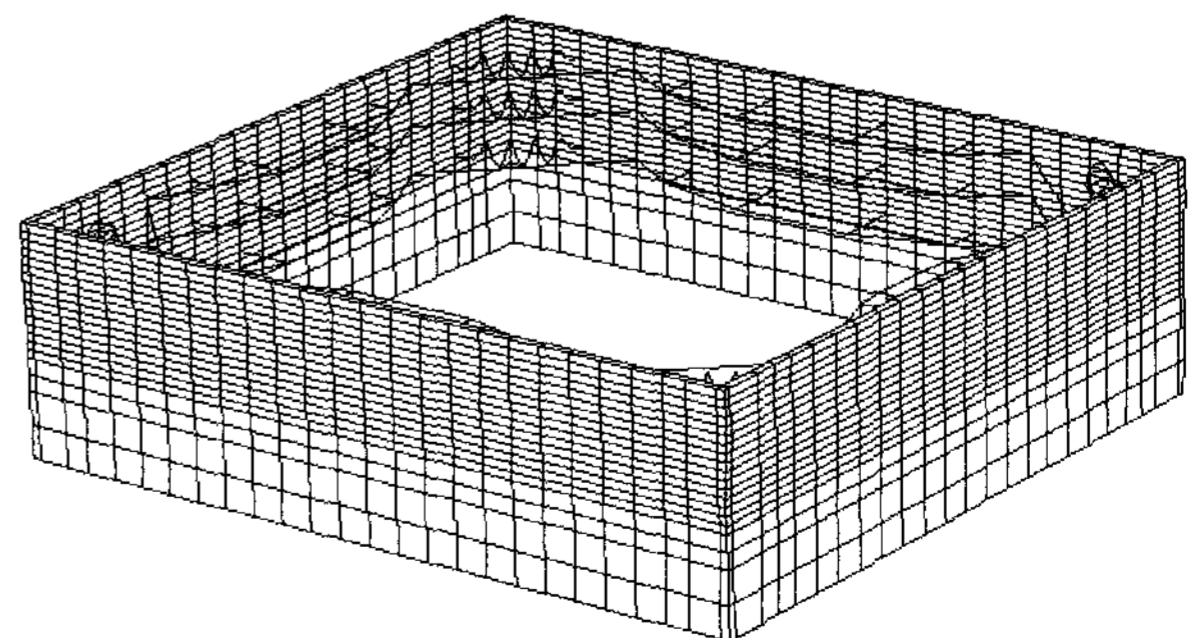


Fig. 5. Finite element mesh of wall and prestressed wale system

3.1.2 Soil and Rock Element Model

The soil and rock were simulated with 3D eight-noded solid elements. The soil and rock were assumed to be elasto-plastic material obeying the Drucker-Prager failure criterion available in ABAQUS (ABAQUS 2004), a commercial FE program. The strength parameters of soil deposits are computed by using the Mohr-Coulomb strength parameters of friction angle ϕ and cohesion c in conjunction with the Drucker-Prager model parameters of β and d (ABAQUS 2004). The strength parameters of the rock mass to perform the finite element analysis were calculated by using the Hoek and Brown criterion (Hoek and Brown 1988). The stiffness of the soil and rock was calculated based on an empirical relationship reported by Janbu (1963). The modeling of the groundwater was not considered in the finite element analysis because the groundwater was not encountered at the site during excavation. The soil and rock material properties examined in the finite element analysis are tabulated in Table 1.

3.1.3 Excavation Support System Model

The CIP wall was simulated with 3D eight-noded solid elements. This solid model was treated as a linear elastic material. The flexural stiffness for the simulated wall was an EI value of the CIP wall in this case history (Kim et al. 2005b). The strut was modeled with two-noded spring elements. In the modeling of the prestressed wale system consisting of wale, support leg, and steel wires, the wale and support leg were modeled with two-noded beam elements. The steel wires were modeled with two-noded truss elements. The material properties of members of the prestressed wale systems and struts are tabulated in Table 2.

3.1.4 Wall-Soil and Wall-Wale Interface Model

The interface of wall-soil and wall-wale was modeled with 2D zero thickness interface model available in ABAQUS. The interface of wall-soil and wall-wale was simulated by the Coulomb friction model provided in ABAQUS. As can be seen in Fig. 6 (a), the proposed

Table 1. Soil and rock material properties examined in finite element analysis

Material	γ (kN/m ³)	ν	E (kPa)	β (degrees)	K	ψ (degrees)	σ_c (kPa)
Fill	18.6	0.3	15,000	50.194	1.0	8.0	16.974
Silty clay with sand	17.6	0.3	25,000	48.065	1.0	6.0	48.930
Weathered soil	19.6	0.3	35,000	52.157	1.0	6.0	53.039
Weathered rock	21.6	0.3	1.78×10^6	54.814	1.0	6.0	112.954

Note: γ is unit weight. ν is Poisson's ratio. E is modulus of elasticity. β is material angle of friction in the $P-t$ plane. K is the ratio of the flow stress in triaxial tension to the flow stress in triaxial compression. ψ is dilation angle in the $P-t$ plane. σ_c is uniaxial compression yield stress. Here, ψ values used in this analysis were referenced from the studies by Bolton (1986), Jewell (1989), and Perkins and Madson (2000). The soil and rock material properties were calculated and based on the results of the field tests.

Table 2. Parameters of members of Earth Retention System for finite element analysis

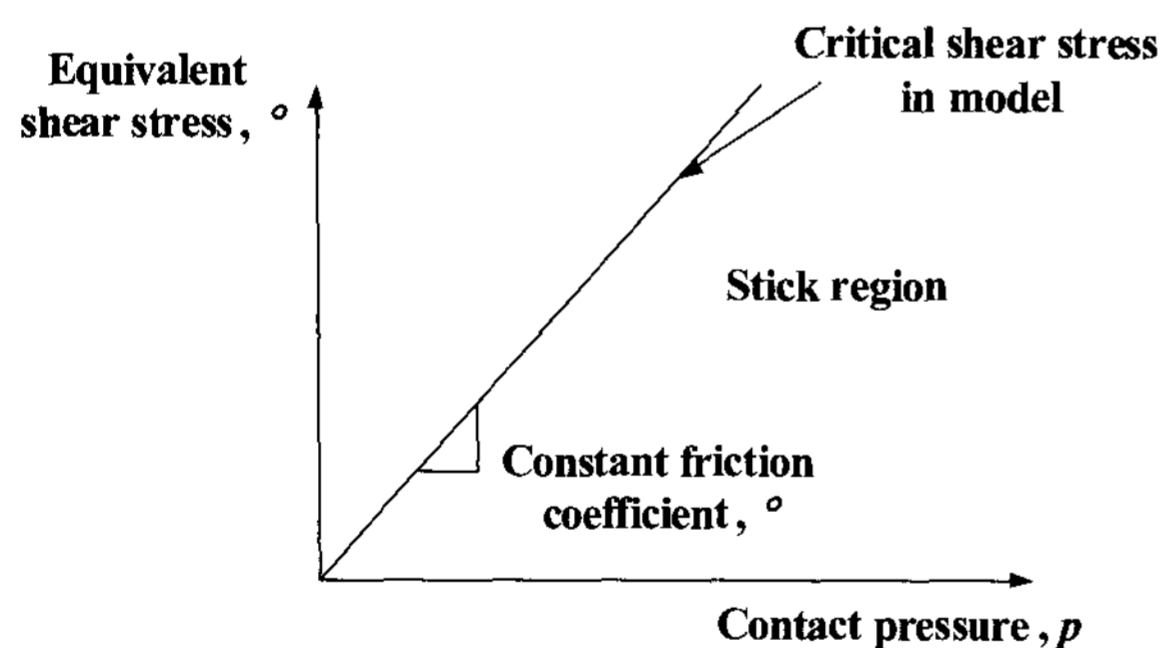
Data	Parameter		Value
Wall	Thickness (m)		0.5
	Height (m)		14.0
	Flexural stiffness (kN·m ² /m)		4.4×10^4
IPS wale No. 1, 3	Length (m)		28.0
	1 st floor	Flexural stiffness (kN·m ²)	5.27×10^6
	2 nd and 3 rd floor	Flexural stiffness (kN·m ²)	8.15×10^6
IPS wale No. 2, 4	Length (m)		22.0
	1st floor	Flexural stiffness (kN·m ²)	2.68×10^6
	2 nd and 3 rd floor	Flexural stiffness (kN·m ²)	3.27×10^6
Corner strut	1 st floor	Axial stiffness (kN/m)	2.11×10^7
	2 nd and 3 rd floor	Axial stiffness (kN/m)	3.07×10^7

model defines the critical shear stress $\tau_{crit} = \mu p$, where μ = constant friction coefficient, and p = contact pressure. Constant friction coefficients of $\mu = 0.2$ for the interface between the soil and the wall and $\mu = 0.3$ for the interface between the wall and the wale were examined in the analyses.

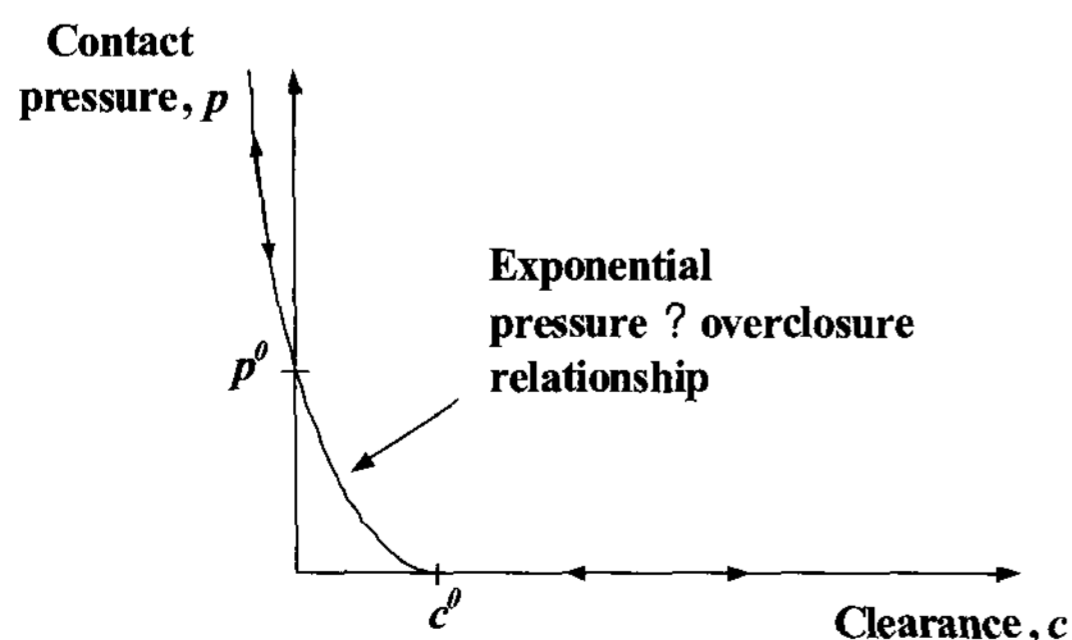
For modeling on the normal behavior of soil-wall and wall-wale interface, as shown in Fig. 6 (b), a contact model to define an exponential contact pressure-overclosure relationship was used in the analyses. For the soil-wall interface modeling, the soil confining pressure of σ_3 was used as the contact pressure p^0 . For the wall-wale interface modeling, the pressure of vertical component in a tensioning force of steel wires was used as the contact pressure p^0 . The clearance c^0 ranging between 10^{-2} and 10^{-4} m was examined in the finite element analyses.

3.1.5 Simulation of Construction Sequence

The simulation sequence for construction activities are shown in Fig. 7. The first step was to turn the gravity stresses on the entire solid, which was 144 m in length, 140 m in width, and 26.4 m in depth. The second step



(a) Friction model



(b) Contact pressure-overclosure relationship

Fig. 6. Interface model

was to install the CIP walls and was to activate the solid elements simulating the wall. The third step was to excavate the soil mass to 3.5 m in depth. The fourth step was to install and prestress the IPS wale systems at the first row. This step consisted of activating the beam elements simulating the IPS wale systems and simulating nodal forces to the wales and support legs, respectively. The fifth step was to install the corner struts at the first row. This step consisted of activating the beam elements simulating the corner struts. The sixth step was to excavate the next soil mass to 5.5 m in depth. The seventh step continued with repetitions of Step 4 to simulate the prestressed wale system at the second row. Total run required about 12 hr of processing on the personal computer with 2GB RAM.

3.1.6 Calibration of Numerical Model

The calibration of 3D finite element model was performed to best match the measured and the calculated. The calibration process consisted of finding the model for wall, strut, and members of the prestressed wale system that led to the best match between the measured and calculated wall deflection. The cast-in-place (CIP) wall was modeled and replaced with rectangular type brick element with equivalent stiffness (AE and EI). For the prestressed wale system modeling, the rectangular beams with equivalent stiffness (AE and EI) were included with the wales, the support legs, and the struts.

3.2 Comparison with Full Scale Experiment

3.2.1 Lateral Wall Deflection

The comparison between numerical predictions and

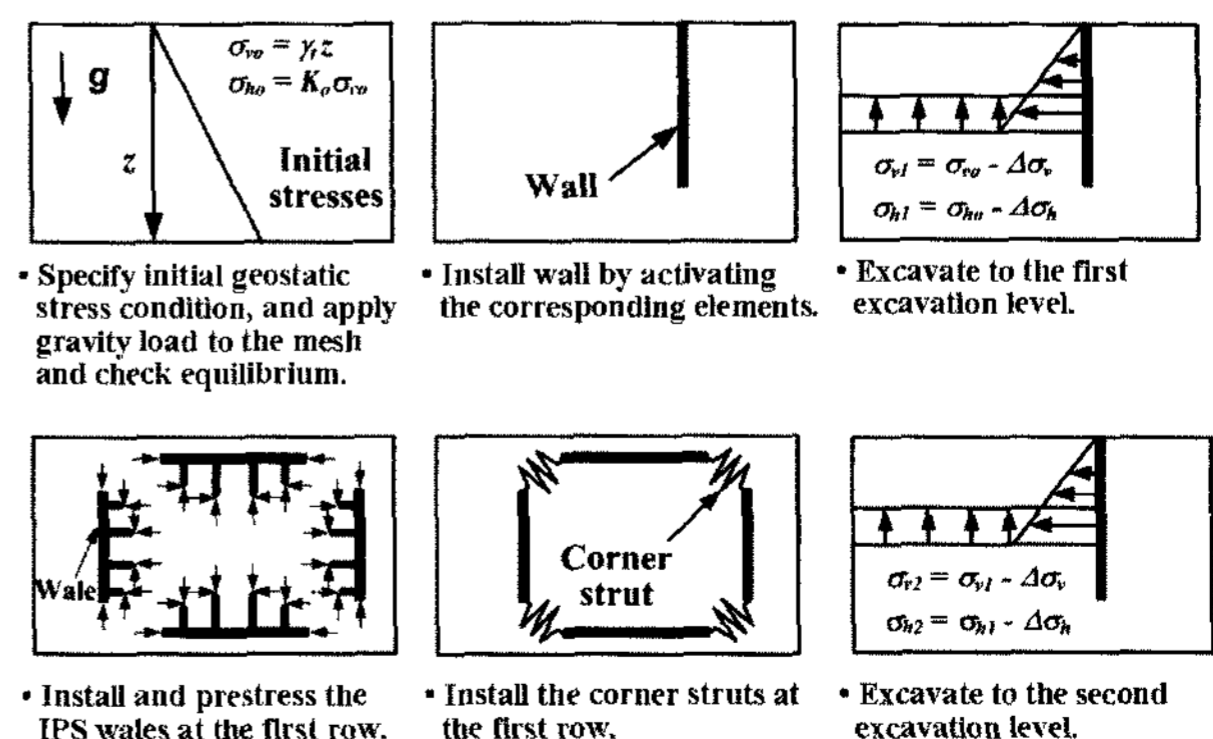


Fig. 7. Simulation of construction activities

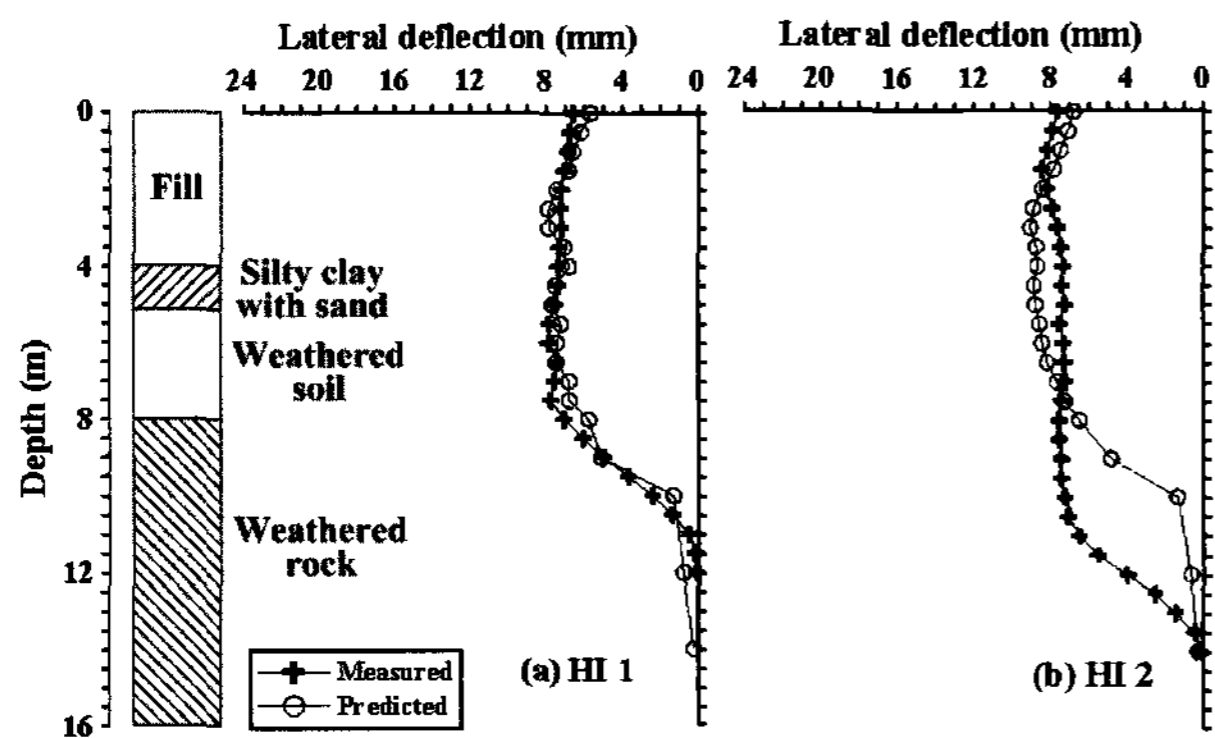


Fig. 8. Comparison between predictions and measurements for lateral wall deflection

measurements for lateral wall deflection are shown in Fig. 8. The lateral wall deflection profiles of HI 1 matched well within 0-13% errors, as shown in Fig. 8 (a). The predicted lateral wall deflections of HI 2 overestimated the deflection 18% larger than the measurements, as shown in Fig. 8 (b).

3.2.2 Axial Load of Wale

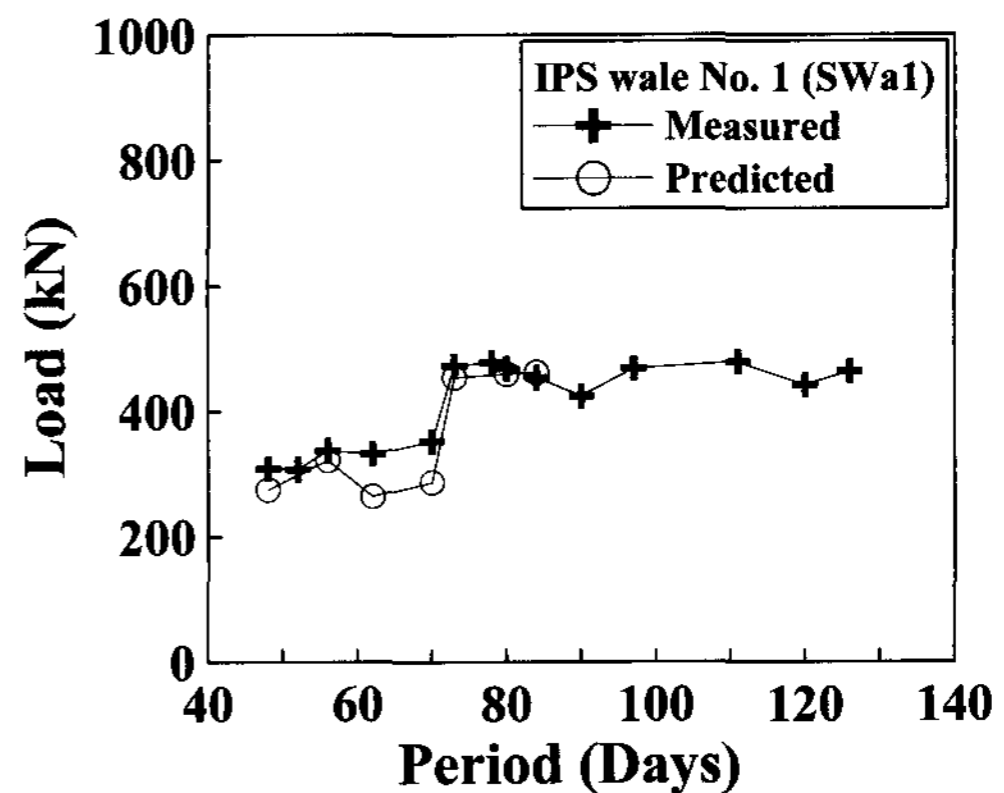
The numerical predictions for axial load of wale of the prestressed wale system were compared with the measurements, as shown in Fig. 9. The predictions of axial load of the wale of the prestressed wale No. 1 at the first to third level gave a correlation with the measurements within 0-20% errors, as shown in Fig. 9.

3.2.3 Axial Load of Support Leg

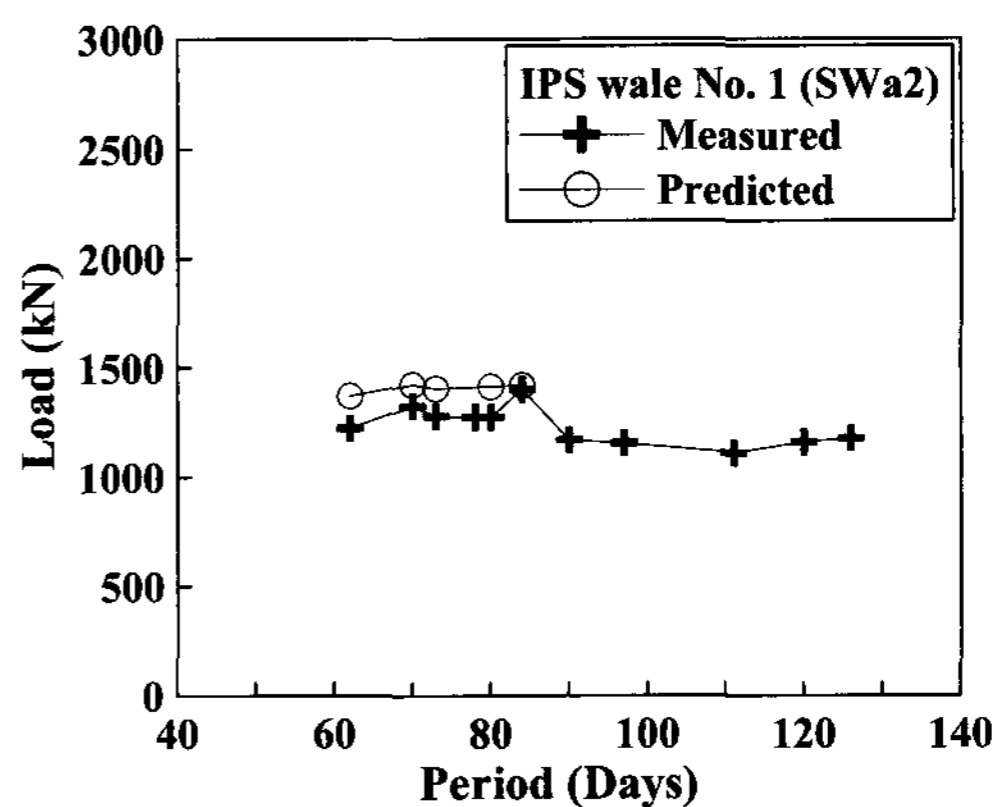
The comparison between numerical predictions and measurements for axial load of support leg are shown in Fig. 10. The predictions of axial load of support legs of the IPS wale No. 1 at the second level and No. 3 at the third level overestimated the load 10.2-25.5% larger than the measurements, as shown in Fig. 10.

3.2.4 Axial Load of Strut

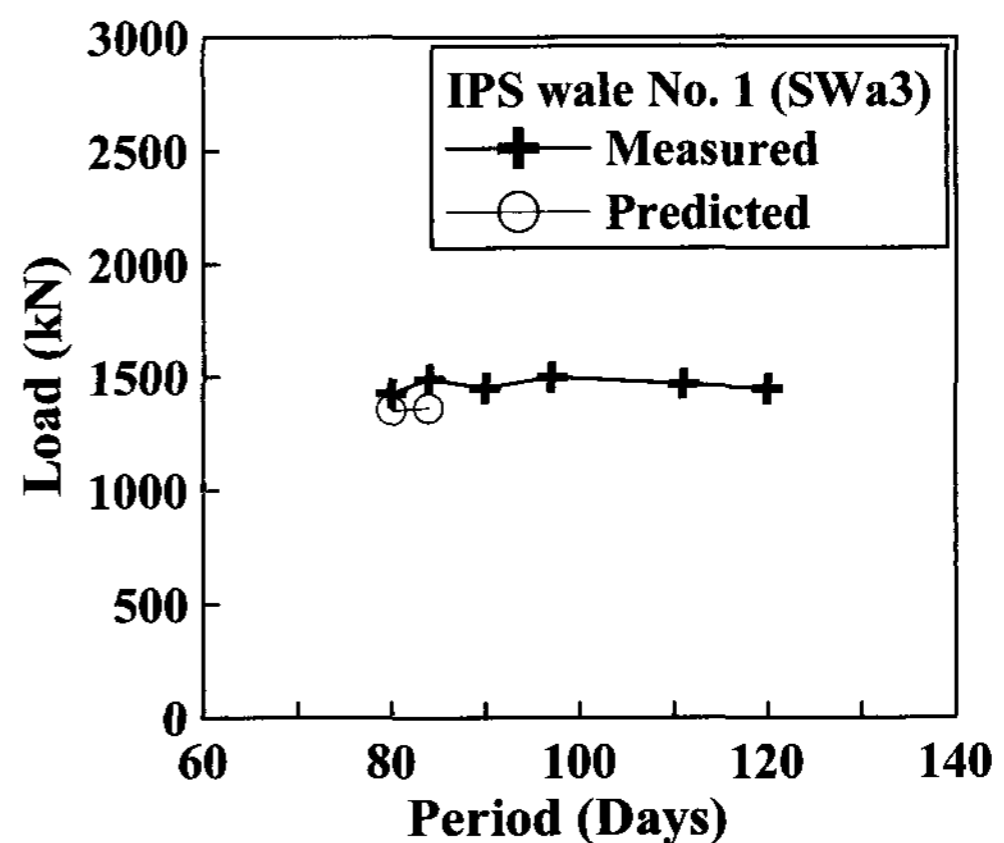
The predicted axial loads of corner strut were compared with the measured data, as shown in Fig. 11. The predictions of corner struts at the first and the third level gave a correlation with the measurement within 9-21% errors, as shown in Fig. 11.



(a) axial load of wale at the first level



(b) axial load of wale at the second level

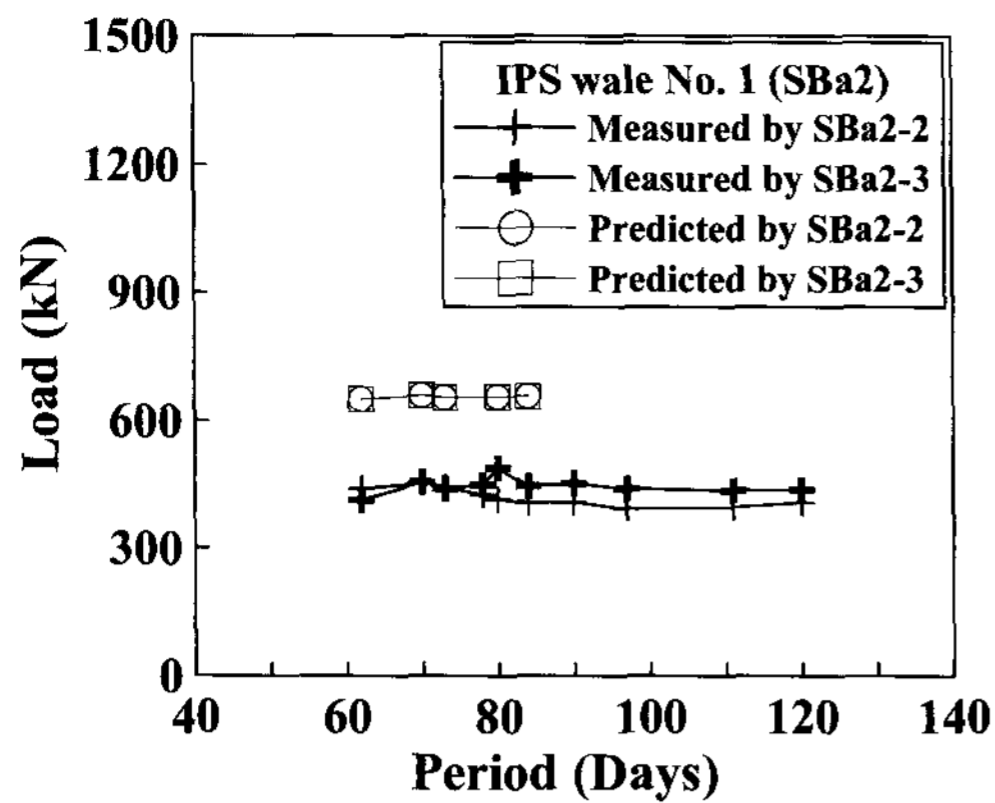


(c) axial load of wale at the third level

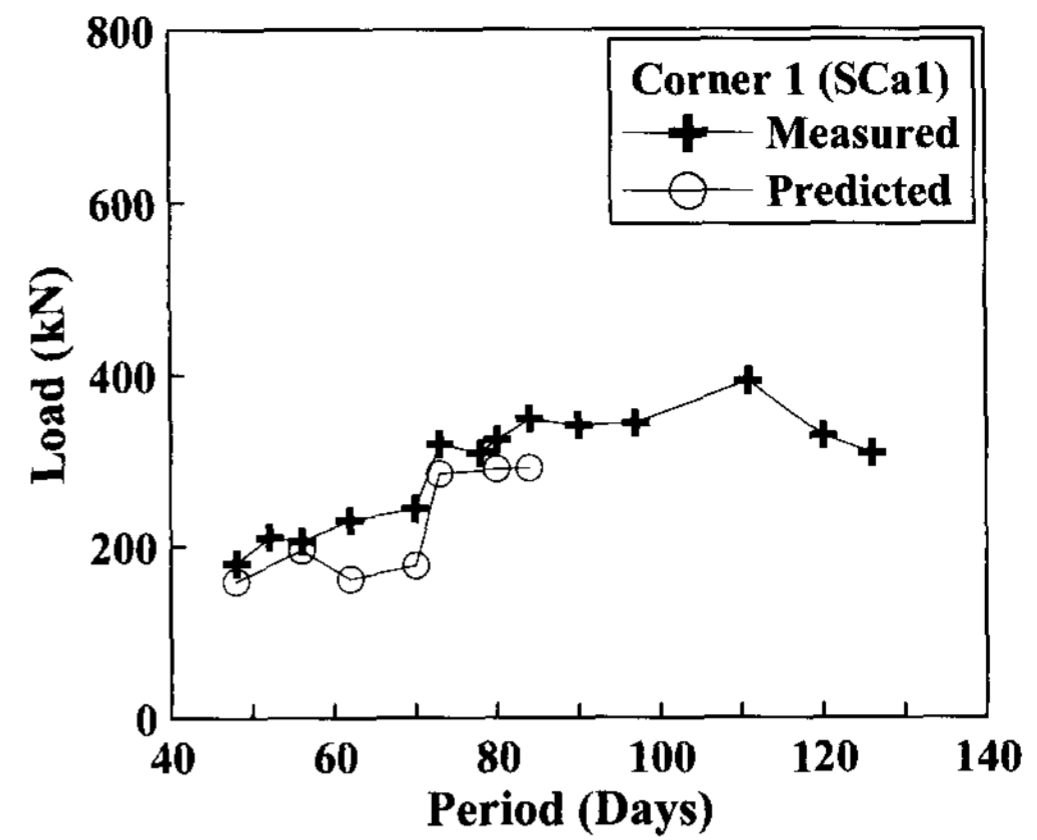
Fig. 9. Comparison between predictions and measurements for axial load of wale

4. Sensitivity Analysis of New Earth Retention System with Prestressed Wales

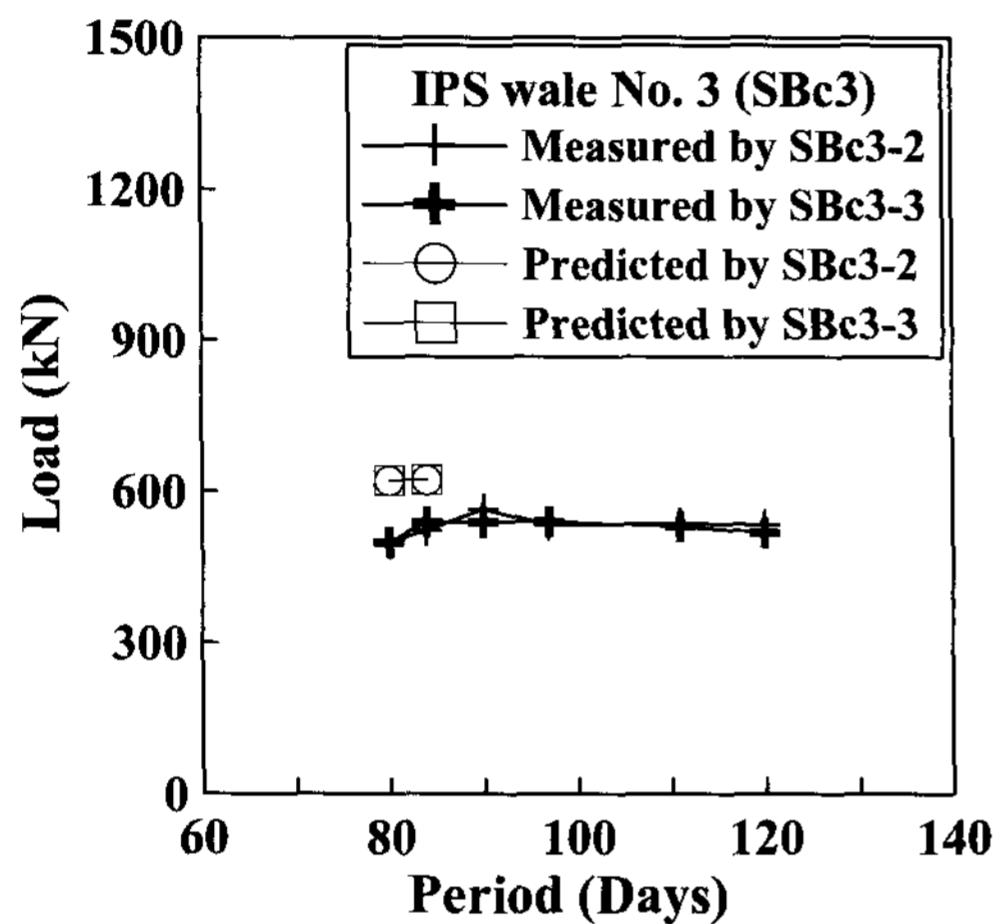
The sensitivity analysis was performed for the new earth retention system with prestressed wales by the finite element method. The prestress load on the new wale system was examined in the finite element analysis to



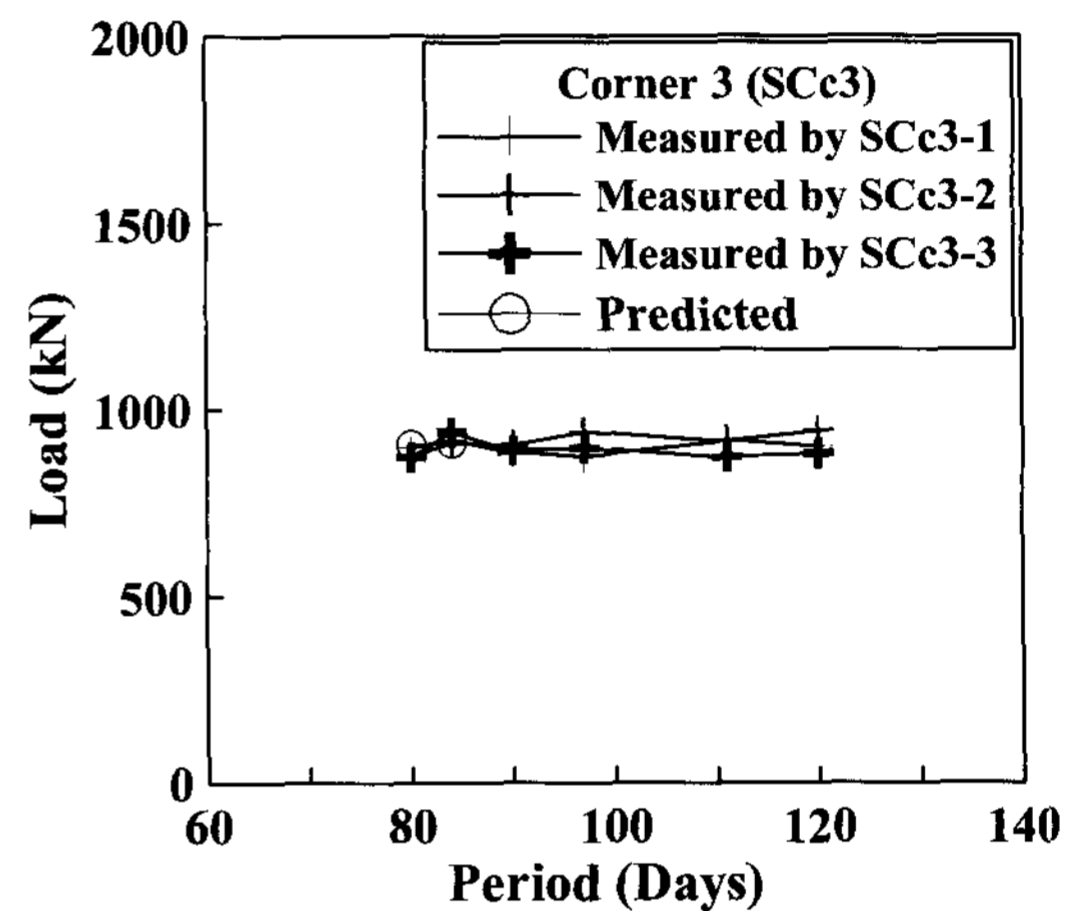
(a) axial load of support leg at the second level



(a) axial load of corner strut at the first level



(b) axial load of support leg at the third level



(b) axial load of corner strut at the third level

Fig. 10. Comparison between predictions and measurements for axial load of support leg

Fig. 11. Comparison between predictions and measurements for axial load of corner strut

evaluate the influence on the lateral deflection of the wall and wales, and the lateral earth pressure distribution on the wall.

4.1 Parameter Examined in Analysis

The prestress load of steel wires was selected as the parameter for the sensitivity analysis of the earth retention system with prestressed wales. The value of the parameter used for the finite element analysis of the earth retention system with prestressed wales is as follows: 1) the value of the prestress load of steel wires was selected as no prestress load, and 50%, 75%, 100%, and 120% of the design tension load of steel wires. The soil properties shown in Section 3.1.2 were used for the sensitivity analysis.

4.2 Sensitivity Analysis Results

4.2.1 Lateral Deflection of Wall and Wale

The lateral wall deflection profiles on the mid-span of the prestressed wale systems at the final construction stage are shown in Fig. 12. The prestress load varied from 0 to 120% of the design tension load of steel wires. As can be seen in Fig. 12, the lateral wall deflection decreased by increasing the prestress load. The wall at the location of the prestressed wale systems significantly deformed back the retained ground by increasing the prestress load. The wall deflection ϕ_{max} by applying prestress load to 120% of the design tension load of steel wires was 1.9% smaller than those of the design load. The wall deflection ϕ_{max} by applying prestress load to 50% and 75% of the design load was 15% and 45%, respectively, larger than those of the design tension load

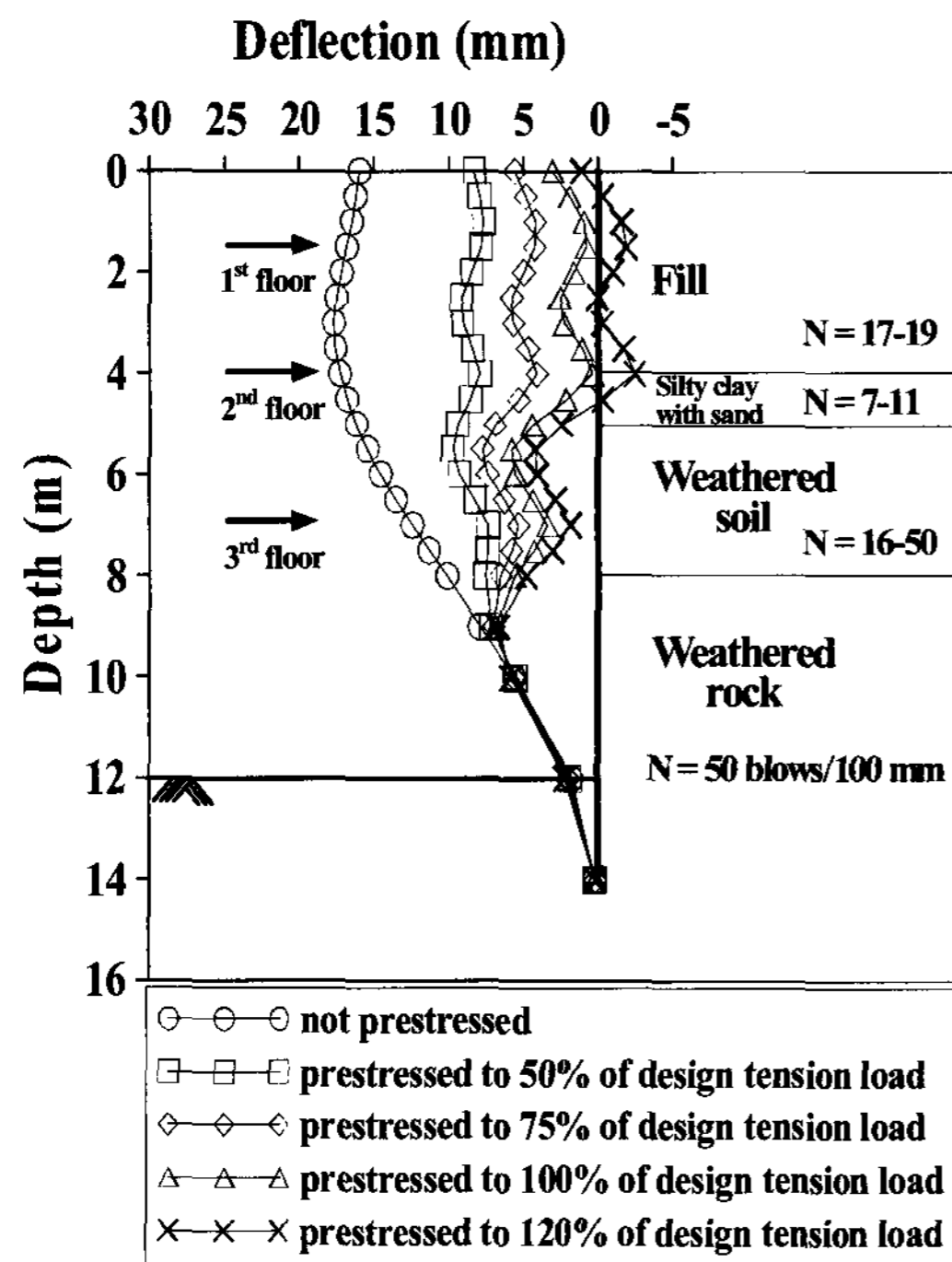


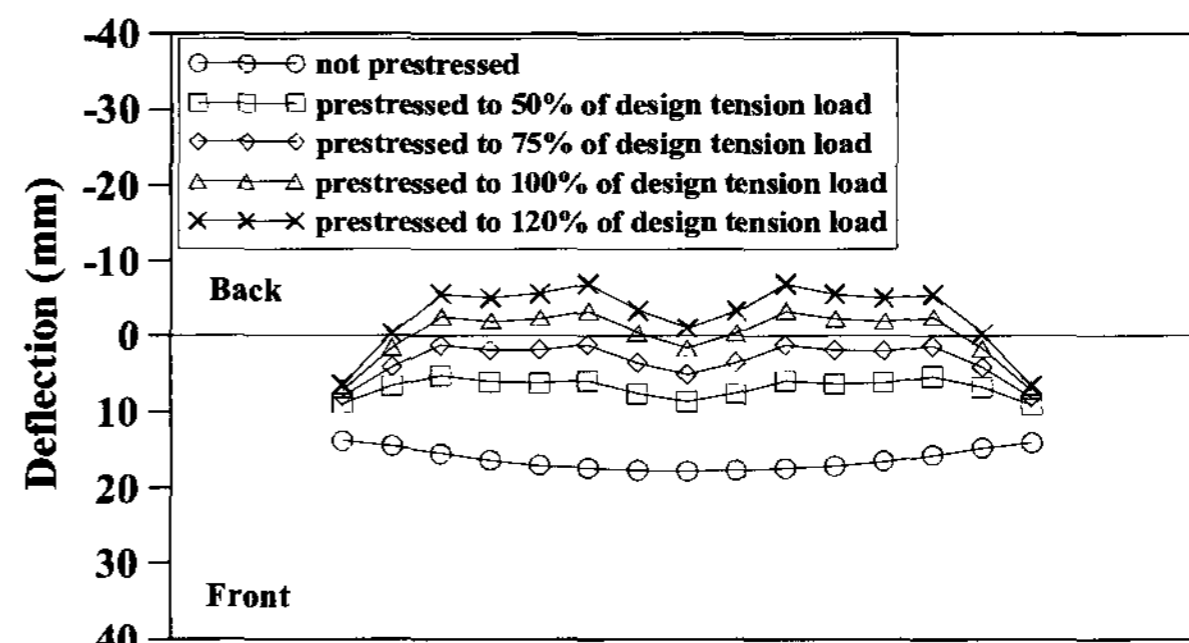
Fig. 12. Variation of lateral deflection of wall

of steel wires.

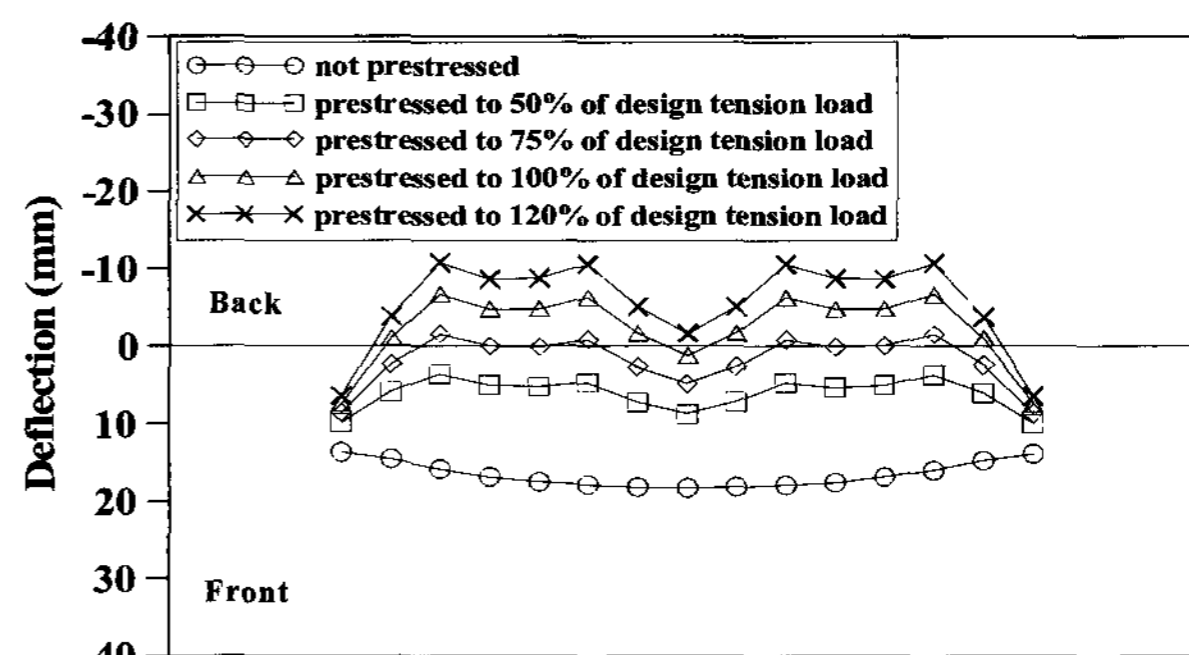
The lateral deflections of the prestressed wale installed at each level at the final construction stage are shown in Fig. 13. The prestressed wale gradually moved toward the retained ground by increasing the prestress load. The wale at the location of support legs significantly deformed back the retained ground by increasing prestress load. The wale at the location of struts was not nearly deformed by large axial stiffness of the strut. The wale prestressed to 120% of the design load of steel wires moved back the retained ground with the deflection of 44% smaller than those of the design tension load of steel wires. The wale prestressed to 50% and 75% of the design load moved back the retained ground with the deflection of 16% and 33%, respectively, larger than those of the design tension load of steel wires.

4.2.2 Bending Moment of Wale

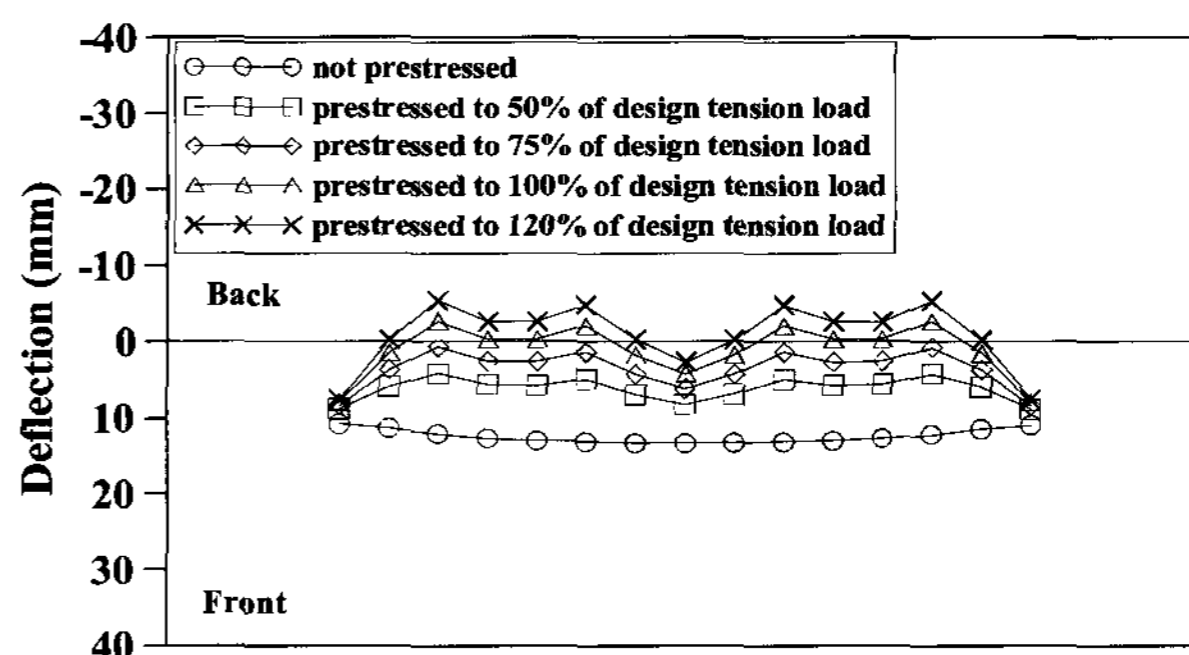
The bending moments of the prestressed wale installed at each level at the final construction stage are shown in Fig. 14. As can be seen in this Figure, the bending moment of the prestressed wale increased with increasing the prestress load. The maximum bending moment of the wale occurred at the location of the outer legs of the



(a) lateral deflection of the wale at the first level



(b) lateral deflection of the wale at the second level



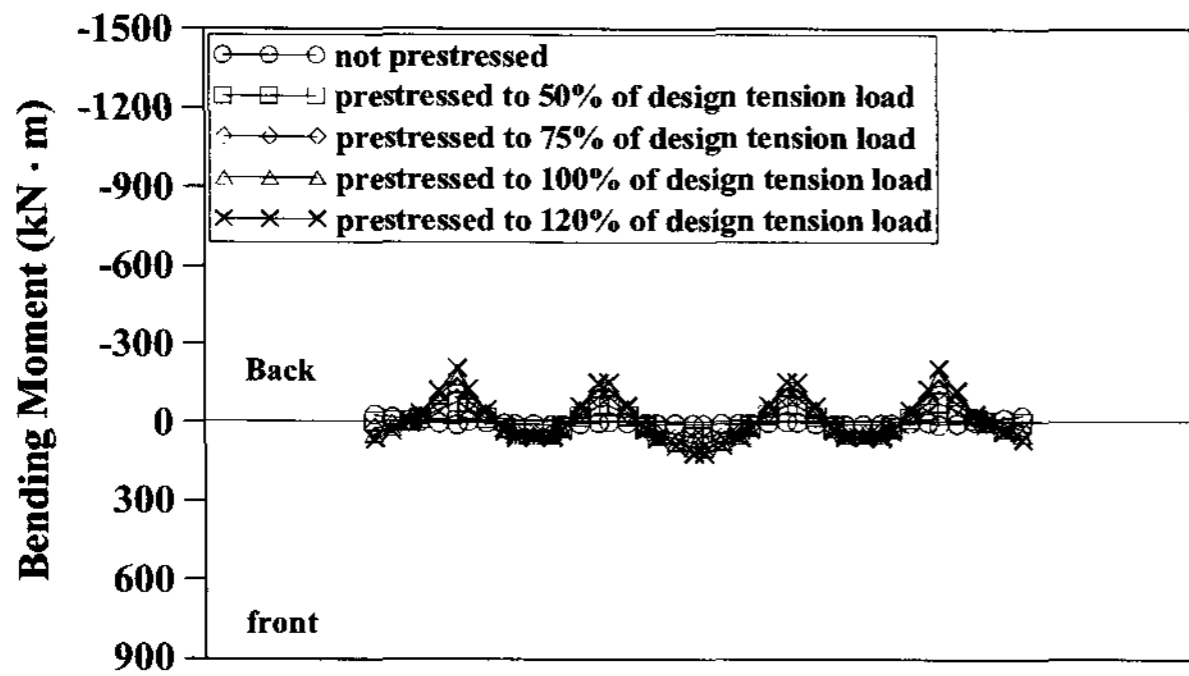
(c) lateral deflection of the wale at the third level

Fig. 13. Variation of lateral deflection of wale

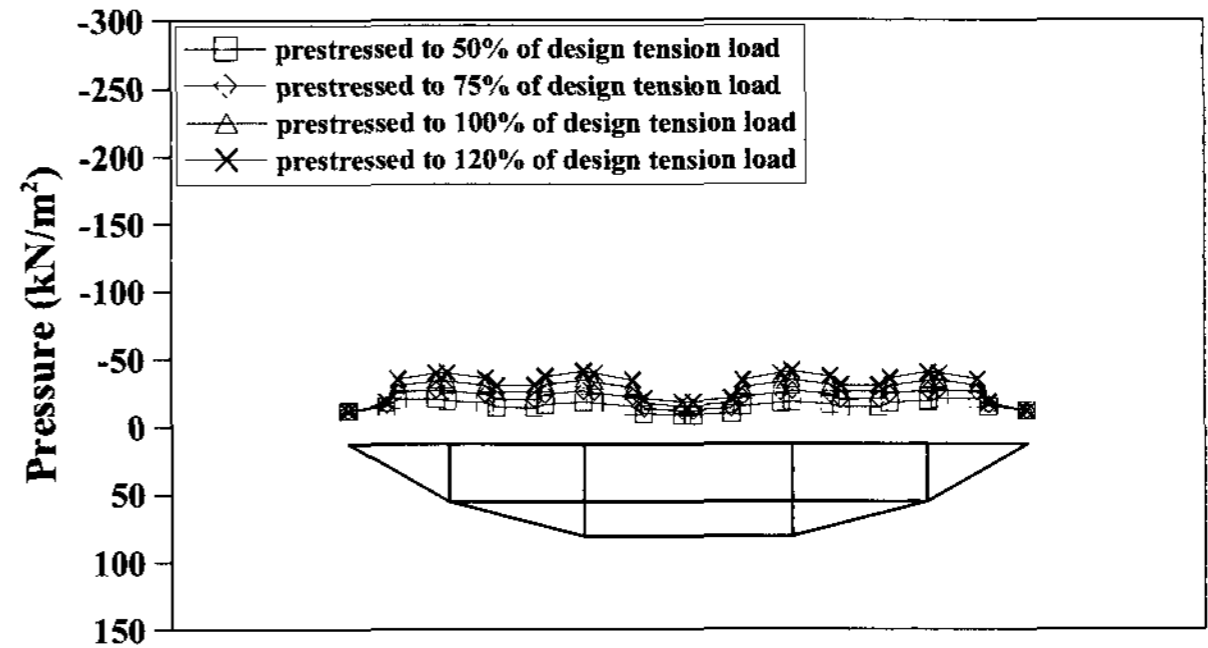
prestressed wale system. The bending moment M_{max} by prestressing to 120% of the design tension load of steel wires was 20.5% larger than those of the design tension load. The bending moment M_{max} by prestressing to 50% and 75% of the design tension load was 25.6% and 51.3%, respectively, smaller than those of the design tension load.

4.2.3 Lateral Earth Pressure on Wall

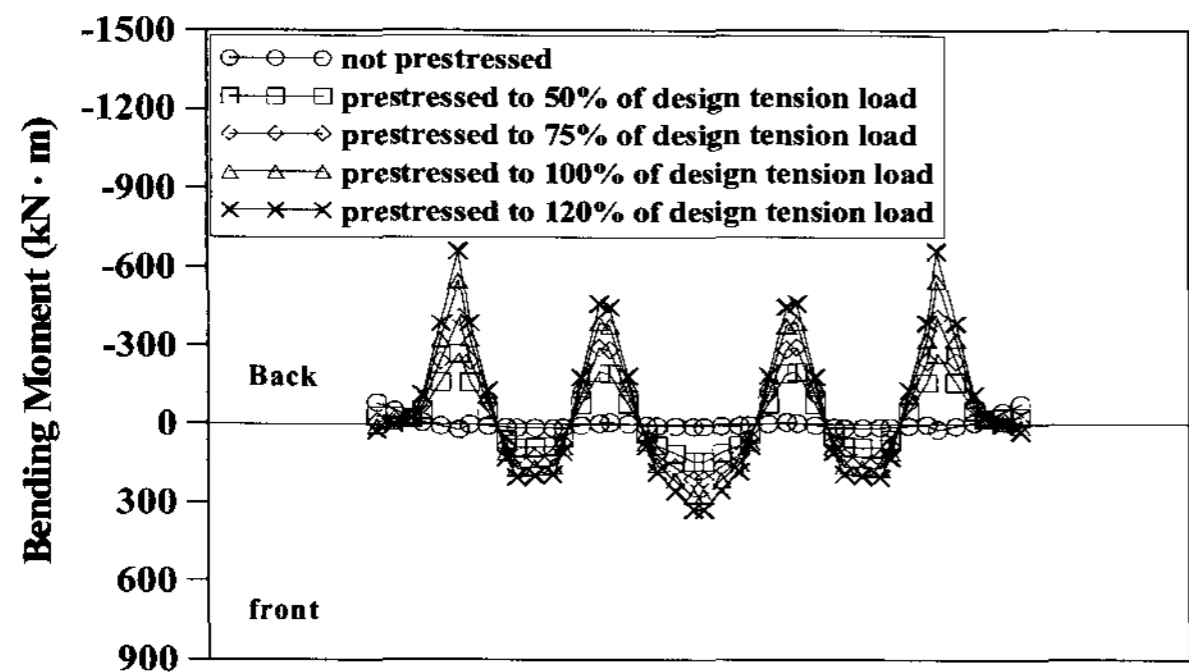
The lateral earth pressure distributions acting on the wall along the prestressed wale installed at each level at the final construction stage are shown in Fig. 15. As can be seen in Fig. 15, the lateral earth pressure on the wall increased with increasing the prestress load. The maximum



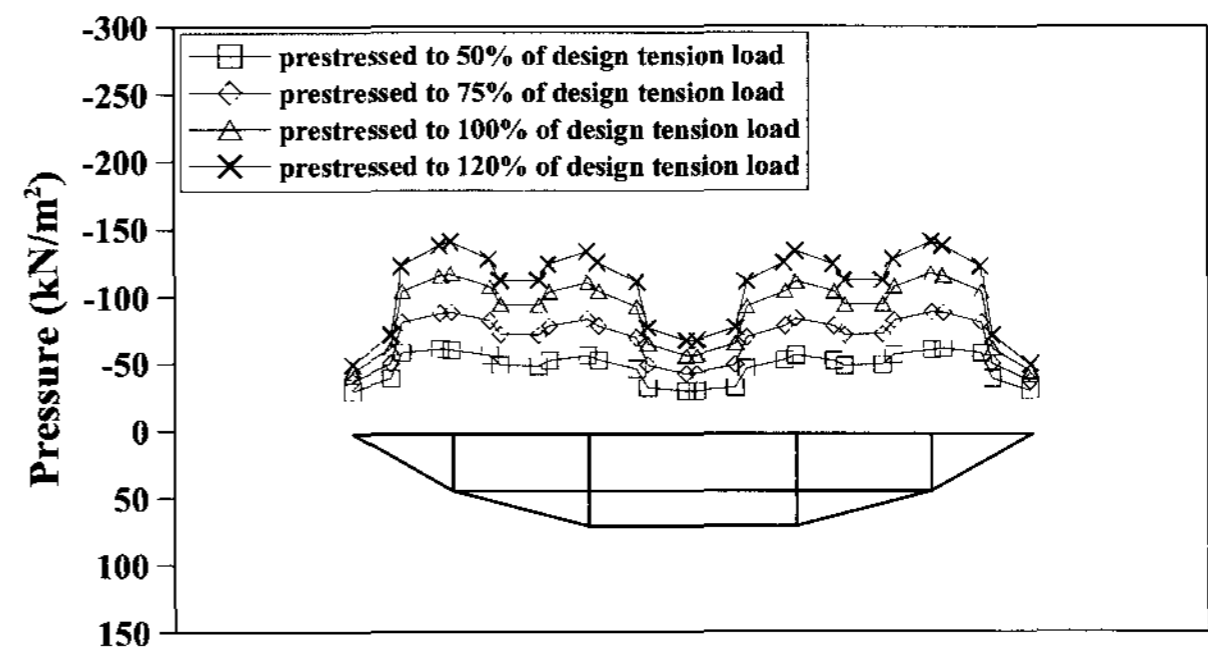
(a) bending moment distribution of the wale at the first level



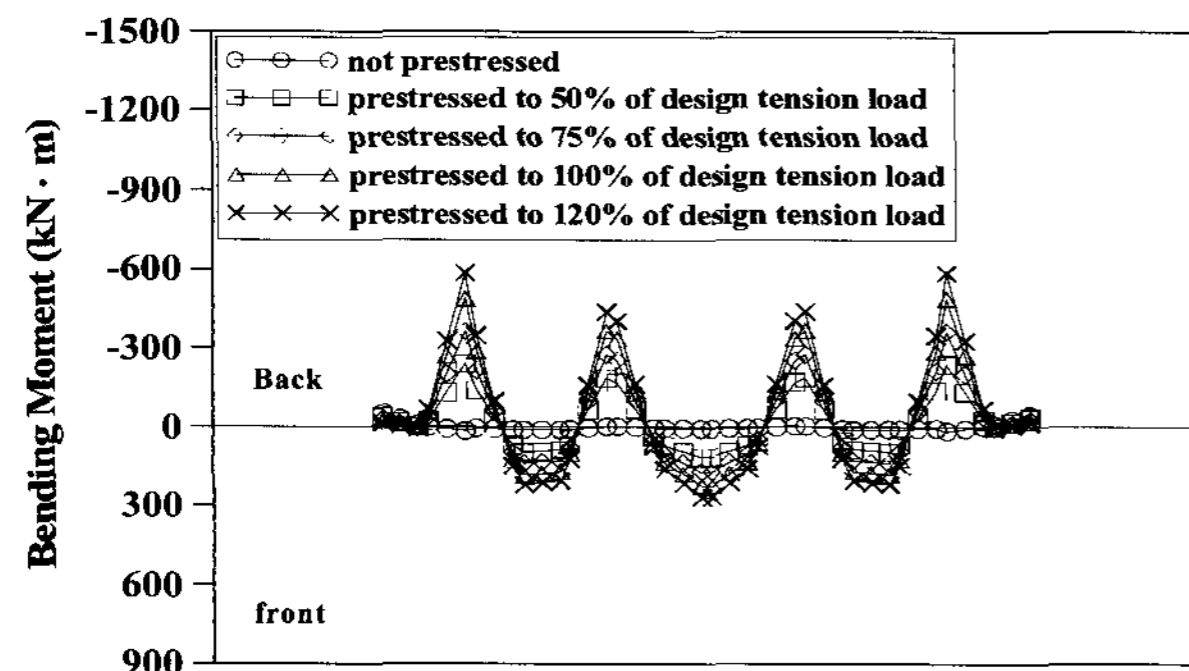
(a) lateral earth pressure distribution on the wall at the first level



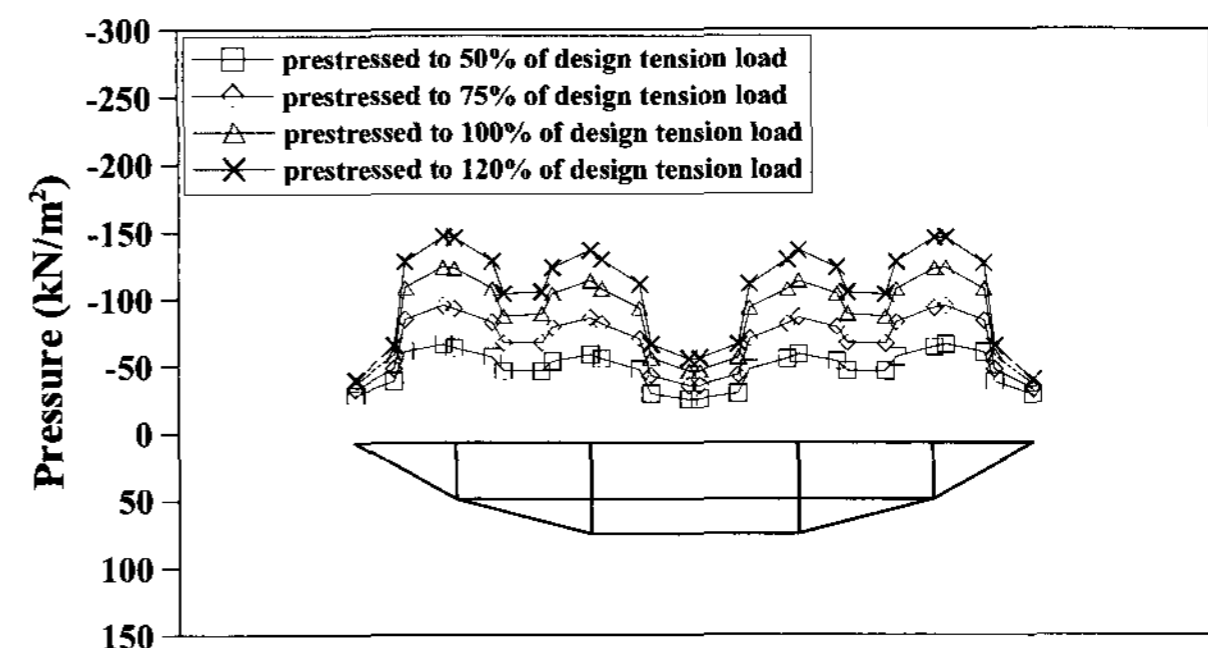
(b) bending moment distribution of the wale at the second level



(b) lateral earth pressure distribution on the wall at the second level



(c) bending moment distribution of the wale at the third level



(c) lateral earth pressure distribution on the wall at the third level

Fig. 14. Variation of bending moment distribution of wale

Fig. 15. Variation of lateral earth pressure distribution on wall

lateral earth pressure occurred at the location of the outer support legs of the prestressed wale system. The lateral earth pressure on the wall at the location of the support legs significantly increased by increasing the prestress load. The maximum earth pressure p_{max} by prestressing to 120% of the design tension load of steel wires was 20.2% larger than those of the design tension load of steel wires. The maximum earth pressure p_{max} by prestressing to 50% and 75% of the design load of steel wires was 24.6% and 47.8%, respectively, smaller than those of the design tension load of steel wires.

5. Conclusions

A 3D finite element analysis was performed to investigate the behavior of the new earth retention system with prestressed wales. Details of the finite element modeling of the earth retention system with prestressed wales were presented. The numerical predictions on the members of the new earth retention system were evaluated compared with the measurements obtained from field instruments. For sensitivity analysis, the prestress load on the new wale system was examined in the finite element analysis to evaluate the influence on the lateral deflection of the wall

and wale, the bending moment of the wale, and the lateral earth pressure distribution on the wall. The following conclusions can be drawn:

- (1) The finite element method can be used to simulate a behavior of the new earth retention system with prestressed wales. The predicted and measured results showed that the lateral wall deflections matched well with 0-18% errors, that the axial loads of the wales gave a correlation with the measured data within 0-20% errors, that the axial loads of the struts gave a correlation with the measured data within 9-21% errors, and that the axial loads of the support legs well matched with the measured data within 10.2-25.5% errors. The numerical error was due to simplifications such as idealization of construction activities, unreal numerical parameters, and excavation geometry.
- (2) Based on the numerical results, the lateral deflection and the bending moment of the wale, and the distribution of lateral earth pressure acting on the wall along the prestressed wales were investigated. It was recognized that the behavior of lateral wale deflection had a relationship with the lateral earth pressure distribution on the wall.
- (3) The behavior of the lateral deflection of the wall and wale, the bending moment of the wale, and the lateral earth pressure distribution on the wall on the effect of the prestress load of steel wires was investigated. From the sensitivity analysis results, it was notified that the prestress load significantly had an influence on the behavior of the wall and wale.

Acknowledgments

This work was supported by grant No. (R01-2003-000-11630-0) from the Basic Research Program of the Korea Science & Engineering Foundation.

References

1. *ABAQUS User's and Theory Manuals* (2004), Version 6.5, Hibbit, Karlson & Sorensen Inc., Pawtucket, R.I.
2. Bolton, M. D. (1986), "The strength and dilatancy of sands", *Geotechnique*, Vol.36, No.1, pp.65-78.
3. Briaud, J.-L., and Lim, Y. (1999), "Tieback walls in sand: numerical simulation and design implications", *Journal of Geotechnical and Geoenvironmental Engineering*, ASCE, Vol.125, No.2, pp.101-110.
4. Han, M. Y., Kim, M. Y., Kim, S. B., Min, B. C., and Lee, J. S. (2003a), "Design of innovative prestressed scaffolding system", *Proc. KSCE Annual Conf. 2003*, KSCE, pp.408-413.
5. Han, M. Y., Kim, M. Y., Kim, S. B., and Park, D. H. (2003b), "Theoretical study on flexural stiffness of innovative prestressed wale", *Proc. KSCE Annual Conf. 2003*, KSCE, pp.3754-3759.
6. Hoek, E., and Brown, E. T. (1988), "The Hoek-Brown failure criterion - a 1988 update", In *Rock engineering for underground excavations, Proc., 15th Canadian rock mech. symp.*, (ed. J.C. Curran), 31-38. Toronto: Dept. Civ. Engineering, Univ. of Toronto.
7. Janbu, N. (1963), "Soil compressibility as determined by oedometer and triaxial test", *Proc. Eur. Conf. on Soil Mech. and Found. Engrg.*, Vol.1, pp.19-25.
8. Jewell, R. A. (1989), "Direct shear tests on sand", *Geotechnique*, Vol.39, No.2, pp.309-322.
9. Kim, N. K., Park, J. S., Han, M. Y., Kim, M. Y., and Kim, S. B. (2004), "Development of innovative prestressed support earth retention system", *Journal of the KGS*, Vol.20, No.2, pp.107-113.
10. Kim, M. Y., Lee, J. S., Han, M. Y., Kim, S. B., and Kim, N. K. (2005a), "A Multi-noded Cable Element Considering Sliding Effects", *Journal of the KSSC*, Vol.17, No.4, pp.449-457.
11. Kim, N. K., Park, J. S., Jang, H. J., Han, M. Y., Kim, M. Y., and Kim, S. B. (2005b), "Performance of innovative prestressed support earth retention system in urban excavation", *J. KGS*, Vol.21, No.2, pp.1-10.
12. Kim, N. K., Park, J. S., and Jang, H. J. (2005c), "Stability of Innovative Prestressed wale System Applied in Urban Excavation", *Journal of the KSMI*, Vol.9, No.2, pp.225-235.
13. Kim, S. B., Han, M. Y., Kim, M. Y., Kim, N. K., and Ji, T. S. (2005d), "Analysis and design of wale in innovative prestressed support(IPS) system", *Journal of the Computational Structural Engineering Institute of Korea*, Vol.18, No.1, pp.79-91.
14. Park, J. S., Kim, J. W., Kim, N. K., Lee, Y. S., and Han, M. Y. (2003a), "IPS Earth Retention System I - Basic Principles", *Proceedings of the KSCE Annual Conference 2003*, KSCE, pp.3775-3779.
15. Park, J.S., Kim, J.W., Kim, N.K., Lee, Y.S. and Han, M.Y. (2003b), "IPS Earth Retention System II - Case Histories", *Proceedings of the KSCE Annual Conference 2003*, KSCE, pp.3748-3753.
16. Park, J. S., Kim, N. K., Han, M. Y., and Kim, J. S. (2004), "IPS Earth Retention System", *Proc. KGS Spring Conf. 2004*, KGS, pp.293-300.
17. Perkins, S. W., and Madson, C. R. (2000), "Bearing capacity of shallow foundation on sand: a relative density approach", *Journal of Geotechnical and Geoenvironmental Engineering*, ASCE, Vol.126, No.6, pp.521-530.
18. Yoo, C. (2001), "Behavior of braced and anchored walls in soils overlying rock", *Journal of the Geotechnical and Geoenvironmental Engineering*, ASCE, Vol.127, No.3, pp.225-233.

(received on Oct. 12, 2007, accepted on Jan. 23, 2008)